

Probing Coal Architecture by Magnetic Resonance Microscopy

D. M. Gregory, D. J. Clifford and R. E. Botto

Chemistry Division
Argonne National Laboratory
Argonne, IL 60439

RECEIVED
OCT 13 1999
OSTI

ABSTRACT

Time-resolved MRM investigations of a well-characterized suite of cross-linked polymers have yielded information on the nature of the solvent transport dynamics and mechanical relaxation of the networks. Network response parameters were then used to assess the macroscopic properties and cross-link densities of polymers with the degree of curing. This new approach is presently being developed to elucidate the complex macromolecular nature of coals and the variation with coal rank.

Keywords: magnetic resonance microscopy, polymers, coal, macromolecular structure

INTRODUCTION

The overall goal of our NMR spectroscopy and imaging program at Argonne is to provide both quantitative and spatially resolved information on the chemical and physical properties of coals. Understanding coal structure in relation to coal reactivity is of utmost significance to the future utilization and carbon management concerns of this important resource, as well as being fundamental to new concepts of energy production and storage. Research carried out in our laboratory over the past several years has focused largely on elucidating the physical structure of coal: one important physical property profoundly influencing coal reactivity is the three-dimensional network structure because of its relevance to properties such as cross-link density in relation to coal depolymerization.

Ingress of solvents into polymers and coals has been studied in the past by traditional volumetric or gravimetric methods, which allow only for indirect observation of the swelling process. During the past several years, we have adopted MRM methods for imaging of the protons in a solvent, to obtain 2D images and 1D concentration profiles, from which fundamental aspects of the transport mechanism during the swelling process can be measured quantitatively^{1,4}. The aim of this work ultimately is to utilize solvent and network response

DISCLAIMER

This report was prepared as an account of work sponsored by an agency of the United States Government. Neither the United States Government nor any agency thereof, nor any of their employees, make any warranty, express or implied, or assumes any legal liability or responsibility for the accuracy, completeness, or usefulness of any information, apparatus, product, or process disclosed, or represents that its use would not infringe privately owned rights. Reference herein to any specific commercial product, process, or service by trade name, trademark, manufacturer, or otherwise does not necessarily constitute or imply its endorsement, recommendation, or favoring by the United States Government or any agency thereof. The views and opinions of authors expressed herein do not necessarily state or reflect those of the United States Government or any agency thereof.

DISCLAIMER

Portions of this document may be illegible in electronic image products. Images are produced from the best available original document.

parameters obtained by MRM to assess fundamental properties of the macromolecular system under investigation. Polymer and coal samples have been studied to date.

Earlier work in our laboratory^{3,4} has demonstrated that Fickian and case II diffusion represent the two extremes of solvent transport. Fickian transport is characterized by a gradual solvent profile whose concentration increases as the square root of time, and where the physical state of the polymer changes slowly compared to the speed of solvent ingress. By contrast, case II transport is characterized by a sharp front moving linearly with time, for which network relaxation occurs on a time scale that is fast compared to the diffusion process. Our previous work⁴ has shown that the change in the physical state of the polymer is typically modeled as a glass-to-rubber transition. However, many polymer systems exhibit anomalous behavior. As in case II transport, the solvent modifies the state of the polymer; however, this occurs on a time scale comparable to the diffusion process.

Our recent *in situ* MRM studies show direct evidence for the latter process. To perform these measurements, we took advantage of "contrast" imaging protocols, using protonated and deuterated solvents, and thereby observed physical changes in rubber samples imbibed with solvent. Using contrast-imaging techniques, i.e., employing diffusion weighting or T₂ weighting, we were able to obtain additional information on the polymer network directly. We studied four cross-linked isobutylene/*p*-methylstyrene rubber samples and showed that several NMR parameters correlate directly with cross-link density.

RESULTS AND DISCUSSION

Imaging of Protonated Solvent

Time-resolved imaging of cyclohexane penetration into the rubber samples suggested anomalous swelling behavior. The region in the center of the samples was completely devoid of solvent throughout the swelling process. Although the cyclohexane front retained the original object shape throughout the diffusion process, the solvent front was not completely sharp as would be expected for pure case II behavior.

The velocity of the solvent front also correlated well with cross-link density. The velocity of the front was greatest in samples with lower cross-link density. This result is expected in light of the diffusion coefficient measurements, which showed that cyclohexane diffuses faster in samples with a lower cross-link density.

Although we attained reasonably good fits to the data with a linear function of position of the solvent front (x) vs. time (t), this approach is only completely accurate in the case where the swelling is purely case II. Instead, the data were fit to a generalized function:

$$x = k + v \cdot t^n, \quad (1)$$

where k = constant and v = front velocity. For the entire suite of rubbers, the average value calculated for exponent n ranged from 0.75 - 0.87, which implied the dynamics of swelling are intermediate between Fickian ($n=0.5$) and case II ($n=1$).

MRM images of cyclohexane swelling of a rubber specimen are shown in Figure 1; a diffusion filter was applied prior to imaging for the images on the right. Because the diffusion coefficient of cyclohexane imbibed in the rubber is substantially less than in the bulk, signal from bulk solvent is suppressed. In the diffusion-weighted images, however,

intensity of imbibed solvent is greatest just behind the solvent front. This is in contrast to the unfiltered images, where the signal intensity is approximately uniform throughout the swollen part of the sample. Thus, there is a direct correlation between intensity of pixels in the diffusion-weighted image and absolute magnitude of the diffusion coefficients. Bright regions indicate solvent with correspondingly lower diffusion coefficients.

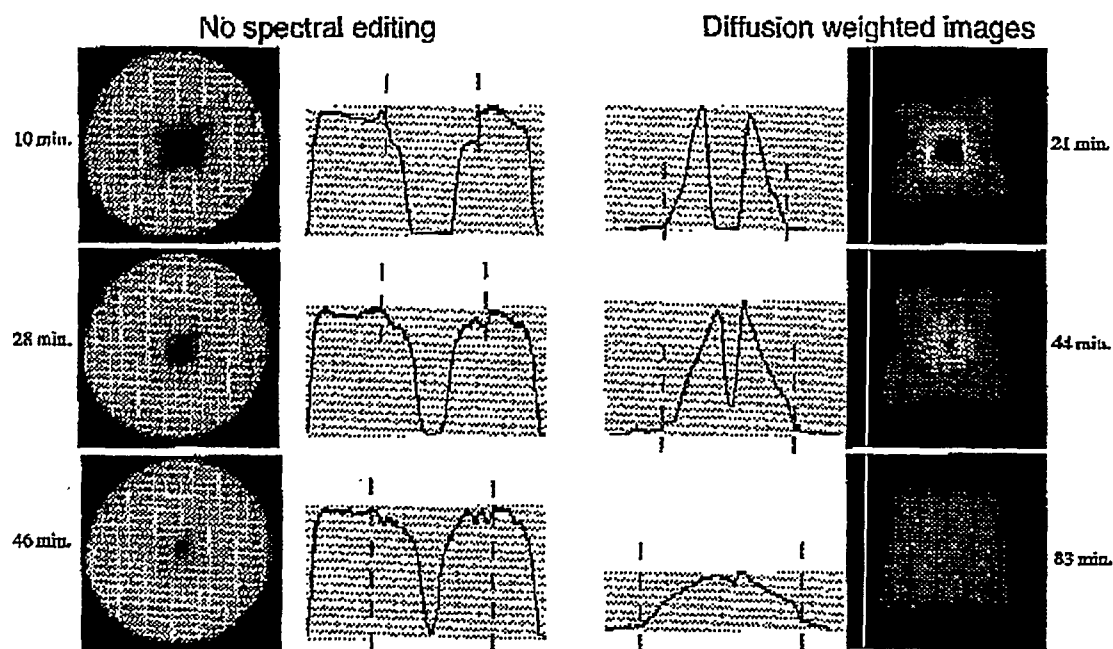


Figure 1. Spin-echo (left) and diffusion-weighted (right) MRM images of rubber specimens.

Moreover, gradation in the diffusion coefficients are perceptible across the swollen samples. The effect is most clearly seen in the 1D profiles. Because the diffusion coefficient is a measure of mean free path, this distance is short for solvent molecules near the solvent front and gradually increases with distance behind the front. This implies that the polymer network continues to expand well after free spaces have been filled with solvent.

Imaging in Deuterated Solvent

By acquiring proton images of the rubber samples during swelling in deuterated cyclohexane, we were able to observe changes in the polymer directly. Conventional spin-echo imaging indicated that the greatest density of polymer occurs near the solvent front. Behind the front, the density of polymer gradually falls off, consistent with the results from diffusion-weighted imaging. Distributional T_2 maps created from the data show a gradation in T_2 values with the shortest T_2 's occurring near the solvent front. This parameter reflects changes in polymer chain motion, i.e., the frequency of chain motion increases gradually from the solvent front.

We also monitored the change in T_2 vs. time for an area of polymer at a constant distance from the outside edge of the sample. The data fit well to a simple exponential function. The 'rate' of change in T_2 for protons in the polymer correlates with cross-link density of the rubber; the rate is slower for samples with higher cross-link density. Final T_2 values show the same trend; samples with higher cross-linking have a lower final T_2 .

Relation to Mechanical Models

We have shown that solvent diffusion coefficients and polymer T_2 values parallel one another, and hence reflect the segmental motions of the polymer chains. These changes take place on a time scale comparable to the diffusion process and are characterized by a single rate constant. At this point it is tempting to try to find analogies between the swelling process that we observe and the mechanical processes commonly measured in polymer systems³. We draw analogy between changes in the motional correlation times of the network and strain relaxation in stress-strain experiments.

In a stress-strain experiment, a constant mechanical stress is applied, and the strain required is measured. In a swelling experiment, a constant osmotic stress is applied by the solvent

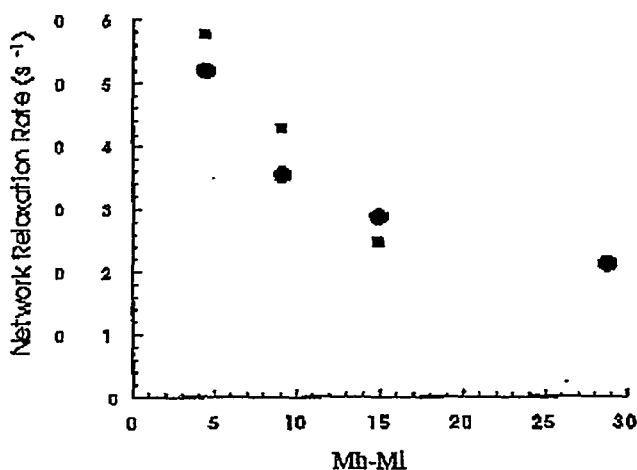


Figure 2. Changes in strain rate from T_2 (circles) and diffusion-weighted (squares) images with cross-link density (Mb-MI) from rheometry torque measurements.

at and beyond the solvent front, and the segmental motion of the polymer chains is measured. In both cases, the strain decreases or relaxes over time. In the simple Maxwell model, the relaxation rate is given by a single exponential. As shown in Figure 2, network relaxation rates measured by T_2 and diffusion-weighted imaging decrease with higher cross-link density of the polymer network.

Preliminary Studies on Coal

MRM images depicting *in situ* swelling of a selected specimen of Pittsburgh No. 8 (APCS 4) vitrain with pyridine are shown in Figure 3. The swelling behavior of this coal is highly anisotropic, with the solvent front moving fastest in a direction perpendicular to the bedding plane. Diffusion of pyridine in this coal is purely case II; the solvent front is extremely sharp, moves at a constant velocity, is linear with time, and has an exponential factor close to unity. Furthermore, bright regions are not observed near the solvent front in diffusion-weighted images, suggesting that network relaxation is on a time scale much faster than solvent diffusion.



Figure 3. Time-resolved MRM of swelling of Pittsburgh No. 8 vitrinite in pyridine.

Future Research

Unraveling the network architecture of coal is fundamentally important to our understanding of coal behavior and reactivity. We plan to perform an NMR imaging study of the solvent transport dynamics and macromolecular network response in Argonne Premium coals. The initial step in this process will be to appraise the dynamic response factors by conducting a systematic study on the suite of three coals of different rank; these are Wyodak (APCS 2), Pittsburgh No. 8 (APCS 4), and Upper Freeport (APCS 1) coals. We also will explore thermodynamic aspects of solvent-solute interactions in these systems by monitoring the solvent and temperature dependence. Data obtained previously on a standard suite of polymers will be used as the model to define parameters that can be used to assess cross-link densities of the coals.

Future work will attempt to compute strain rates from solvent front velocities and network relaxation rates, assuming pure Newtonian viscous behavior. To a first-order approximation, the strain rate can be related to the osmotic stress, i.e., the chemical potential of the solvent in equilibrium with the polymer, by applying Flory-Rehner (F-R) theory, from which parameters such as the number averaged molecular weight between cross-links may be estimated.

Assuming stress is purely osmotic in nature, $\sigma = \Pi$, it follows that for a Newtonian fluid the strain rate

$$de/dt = RT/v_1 \eta \cdot \ln a_1 \quad (2)$$

Using F-R theory we can determine Π at v_2^* , by defining the chemical potential of a solvent in equilibrium with the polymer,

$$\ln a_1 = \underbrace{[\ln(1-v_2) + v_2 + \chi v_2]}_{\text{solvent terms}} + \underbrace{\{Z(v_2^{1/3} + v_2/2)\}}_{\text{entropic constraint}} \quad (3)$$

where $Z = \rho v_1 / \langle M_c \rangle$, ρ is the dry density of the polymer, v_1 is the molar volume of the solvent, and $\langle M_c \rangle$ is the number averaged molecular weight between cross links. In proceeding with this calculation, we have to make numerous simplifying assumptions. Most importantly, we must neglect contributions from hydrogen-bonding equilibria to the chemical potential. These should be most important in the case of coals of low rank. To approximate these interactions, we intend to consider hydrogen bonding effects globally as part of the interaction enthalpy term, i.e., favorable interactions associated with hydrogen bonding being

partially offset by unfavorable solvent-solute interactions, thus yielding adjusted χ values. Secondly, in order to compute the osmotic pressure at v_2^* , one must assume that χ is independent of concentration. Although this is certainly not true, it is unlikely that χ will vary significantly with concentration. Moreover, the third term in equation 5 should not significantly affect Π .

Although the treatment and analysis of MRM strain data is approximate, such an approach does hold promise for assessing macromolecular structure parameters of coal, thus adding to our growing understanding of coal structure/reactivity properties.

ACKNOWLEDGMENTS

This work was performed under the auspices of the Division of Chemical Sciences, Office of Basic Energy Sciences, U. S. Department of Energy under Contract No. W-31-109-ENG-38.

REFERENCES

1. L. Hou, P. G. Hatcher, and R. E. Botto, *J. Coal Geology* **1996**, *32*, 167-189.
2. L. Hou, G. D. Cody, D. C. French, R. E. Botto, and P. G. Hatcher, *Energy Fuels* **1995**, *9*, 84-89.
3. G. D. Cody and R. E. Botto, *Macromolecules* **1994**, *27*, 2607-2614.
4. G. D. Cody and R. E. Botto, *Energy Fuels* **1993**, *7*, 561-562.